Journal of Cultural Heritage 80 (2026) 155–164

Contents lists available at ScienceDirect

Journal of Cultural Heritage

journal homepage: www.elsevier.com/locate/culher

Original article

A design of experiment approach for investigating active fiber lasers: Influence of the adjustable parameters in the cleaning process

Marina Polizzi[a], Francesca Zenucchini[b], Marie-Claire Canepa[b], Alessandro Zanini[c], Laura Bartoli[c], Barbara Giussani[d,*], Dominique Scalarone[a,*]

[a] Chemistry Department, University of Torino, Torino10125, Italy
[b] Fondazione Centro Conservazione e Restauro “La Venaria Reale”, Venaria Reale10078, Italy
[c] Light for Art – El.En. Group, Calenzano, FI 50041, Italy
[d] Science and High Technology Department, University of Insubria, Como 22100, Italy

A R T I C L E I N F O

Article history:
Received 30 December 2025
Accepted 11 May 2026

Keywords:
Yb-doped active fiber lasers
Design of experiment
Parameter influence
High repetition rate
Pulse duration
Scan speed

A B S T R A C T

The use of active fiber lasers for cleaning applications in the field of cultural heritage is in rapid expansion. One of the main potentials of this new technology lies in the possibility to combine a broader range of parameters compared to lamp-pumped lasers, enabling different types of interactions with the materials. In addition, the possibility to choose from a variety of scan shapes and sizes modifies the spatial distribution of the energy on the surface and accelerates the cleaning process.

In this study, a Design of Experiment (DoE) approach was combined to Principal Component Analysis (PCA) to investigate the influence of repetition rate, pulse duration, power and scan speed in the cleaning process. The tests were performed on mock-ups replicating the Roman fresco technique coated both with an organic layer, a *strappo glue*, and an inorganic layer, a *limewash*. A series of responses were selected to evaluate the transformations occurred on the surface after laser irradiation: the changes in surface roughness and color before and after the treatment, and the assessment of the alteration percentage induced on the materials.

The DoE methodology was implemented to define an experimental domain, allowing the evaluation of both the influence and the interactions of the investigated parameters across the entire domain with a preliminary settled and reduced number of tests. The selected responses were analyzed through Principal Component Analysis (PCA), which revealed the underlying correlations among them and permitted the selection of a reduced, yet representative, subset of responses for analysis. Through this integrated approach it was possible to identify the key parameters controlling the two different cleanings, to distinguish those suitable for optimization and to categorize the possible surface alterations that can occur when the parameters are not properly adjusted. Finally, the present study also highlights the differences in the removal of inorganic and organic materials.

1. Introduction

Since the first applications of laser systems in the field of cultural heritage [1,2], lamp-pumped lasers have been the predominant type of laser technology adopted; however, in recent years, a novel form of laser technology, namely active fiber lasers, has emerged as a viable option for a variety of applications. The use of these devices was initially confined to the industrial sector, particularly in the domain of cutting, welding or removing paint layers from large machinery [3,4]. Since then, active fiber lasers have been applied in the cultural heritage field, with the first studies reporting the use of these new systems on an artwork presented at a LACONA conference in 2009 [5,6]. Active fiber lasers have been applied on stone materials [7–10], wall paintings [6,8], plaster [11], wood [8,12] canvas [8,13], carboard [8] and metallic artworks [14,15].

The major potentiality of active fiber lasers is the possibility to select through the user interface a wider range of parameters compared to traditional lasers. Indeed, the parameters that can be modulated are pulse duration, repetition rate, power, scan speed and the shape and size of the scan. The importance of this possibility relies on the fact that different combinations of parame-

* Corresponding authors.
E-mail addresses: barbara.giussani@uninsubria.it (B. Giussani), dominique.scalarone@unito.it (D. Scalarone).

https://doi.org/10.1016/j.culher.2026.05.012
1296-2074/

ters can produce different types of interaction with the materials to be removed and, consequently, different types of cleaning [7]. Furthermore, modulating the shape and the size of the scan influences the spatial distribution of the emitted energy and increases the cleaning speed compared to lamp-pumped lasers. This makes active fiber lasers particularly effective for cleaning large surfaces, such as archaeological sites, façades or statues [9,16].

A distinguishing characteristic of active fiber lasers is that the fluence alone cannot fully account for the energy emitted onto the material. To gain a complete understanding of the energy delivery process on the material, it is necessary to consider the combination of all the selectable parameters. Fiorucci et al. [17] emphasized this aspect and stressed the importance of factoring in repetition rate and scan speed due to their cumulative effects. Therefore, studying the influence of parameters is essential to fully understand how these laser systems work.

Noteworthy, the effect of parameter variation has already been the subject of previous studies. The pulse duration is directly correlated with the definition of thermal irradiation and the depth of the substrate heating [18–20]. At short or medium duration pulses, it is possible to operate under thermally confined conditions, according to the thermal diffusivity of the material. Conversely, longer pulse durations lead to a larger affected volume but with a lower peak temperature compared to short pulses [21–23]. Furthermore, other researches [19,21,22,24] demonstrated that the variation of the pulse duration can result in different laser ablation mechanisms.

The selection of the scan shape and of the repetition rate influences the overlap rate, which is defined as the percentage of overlap between two consecutive spots. Increasing the scan speed while maintaining fixed the repetition rate results in a decrease in spot overlap. Conversely, at a constant scan speed, higher repetition rates lead to a greater overlap. At low scan speeds and repetition rates in the hundreds, overlap is always a dominant phenomenon and the laser exhibits a quasi-continuum behavior [7]. Another critical factor to consider is that, at higher overlap rates, the surface thermal accumulation becomes predominant [25–27]. This occurs because the second pulse arrives before the heat generated by the previous one has fully dissipated [6,18]. More generally, a high repetition rate is recognized as a key contributor to cumulative heating, as highlighted by several studies [19,23,28–30].

Previous studies [17,31] also investigated the impact of the scan speed variation onto the cleaning process, concluding that lower scan speeds were associated with greater laser ablation than higher scan speeds [31].

Moreover, while in lamp-pumped lasers the output energy can be modulated via the control monitor, in active fiber lasers it is possible to select the power percentage, which directly influences the total output energy and average power [14,32].

Principal Component Analysis (PCA) is the most widely employed tool for dimensionality reduction of high-dimensional space data and it is applied to the results of different analytic techniques, such as spectroscopic analysis or hyperspectral imaging. Riu et al. [33] provided an overview of the application of chemometrics in cultural heritage conservation field. PCA is useful for characterizing constituent materials [34–36], as well as for assessing the conservation state of artworks and their degradation products [37–40]. Moreover, it is also applied to study restoration processes [41] and to define the most appropriate sampling points [42]. On the other hand, while the Design of Experiments offers considerable potential for conducting experiments involving multiple variables, it is not yet widely used in the cultural heritage field, with few representative studies available in the literature [43]. Nonetheless, Ouyang et al. [44] applied DoE to optimize the removal of a coating using an active fiber laser in an industrial application.

In this context, the application of DoE in the field of cultural heritage is an innovative way to study the relationships between multiple input and output variables, to reveal correlations and interactions among them, and to gain understanding across the entire experimental domain, and not just at tested points [45]. A key advantage of the methodology proposed in this study is that it allows to maximize the information gained while minimizing the number of experiments, reducing the wasted material and the repetitions. Furthermore, both DoE and PCA were implemented using an open-source software, permitting this approach to be fully accessible and reproducible by other researchers.

2. Research aim

The present study paves the way for a new methodology for testing and validating new cleaning techniques through the combined application of Design of Experiment (DoE) and Principal Component Analysis (PCA). The aim of this research is to investigate the influence of the multiple adjustable parameters, namely repetition rate, pulse duration, power, and scan speed, on the cleaning process when operating with an active fiber laser. Furthermore, this research examines the role of interactions between the different parameters and provides an approach to define a suitable parameter combination to obtain the desired material removal without altering the substrate. It also identifies the possible types of alteration that may occur when the parameters are not properly modulated. Finally, the study focuses on the removal of two different materials, one organic (a *strappo glue*) and the other inorganic (a *limewash*) from *fresco* mock ups, to provide a comparative evaluation for parameter selection during the removal of materials with distinct properties. This approach demonstrated the potential applicability of active fiber laser on polychrome materials, and particularly *frescoes.*

3. Materials and methods

3.1. Materials

3.1.1. Sample preparation

The experiments were conducted on mock-ups designed to simulate traditional Roman *frescoes*. Two layers of lime-based mortar, traditionally referred to as *arriccio* and *intonaco* [46], were applied on an aluminum honeycomb panel. The lime was mixed with marble powder in proportion 1:2.5, using increasingly fine-grained aggregates from the innermost to the outermost layers [47]. Finally, the paint layer was created by diluting Rosso Pozzuoli pigment (PR 102/77,491, Sinopia S.a.s) in water and by applying it with a brush to the fresh surface. The painting layer was then polished with a metallic instrument to make the surface finer, more compact and more resistant, according to the Roman *politiones* technique [48].

After natural ageing of the mock-ups for 2 months to ensure carbonation of the *intonaco,* two overlapping layers were applied using the micrometer adjustable film applicator Sheen 1117/200. The organic layer used in the experiments was a *strappo* glue applied at a thickness of 60 µm, prepared according to the Mora-Philippot receipt, which requires 3 kg of bone glue in pearls, 2.5 kg of water, 0.75 kg of molasses, 2 l of vinegar and 0.3 l of ox bile [49]. The selected inorganic layer was a *limewash*, thickness of 20 µm, applied on top of a fine layer of diluted clay (clay-water ratio 1:10 w/w) with a thickness of 10 µm to replicate a layer of superimposed material.

3.1.2. Laser instrument

The cleaning tests were performed using the active fiber laser Smart 300 (El.En Group). This laser system is Ytterbium-doped

Table 1
Technical features laser Smart 300 (El.En Group).

Type	Value
System	Active fiber laser ytterbium doped
Wavelength	1064 nm
Pulse duration	2–500 ns
Repetition rate	2–4000 kHz
Maximum power/energy emission	300 W/15 mJ
Laser beam diameter at the handpiece output d_{86} (i.e., 86% of the output power)	290 μm
Laser beam divergence full angle d_{86} (i.e., the 86% of the output power)	18 mrad
Beam delivery	5 m optical fiber
Nominal ocular hazar distance (NOHD)	154.2 m

and emits at 1064 nm. Its technical features are reported in Table 1 [50].

During the tests the laser was fixed to a tripod, ensuring a consistent distance of 254 mm between the handpiece and the mock-up, that corresponds to the focal distance of the f-theta lens on the handpiece.

3.2. Instrumentation

Three colorimetric and roughness measurements were carried out in each test section, both before the application of the overlapping layers and after their removal. To ensure the representativeness of the data, the measurements were always performed at the same point using a previously prepared mask. The sampling points were located at the top, center and bottom of each test area.

3.2.1. Colorimetric measurement

Color variations were monitored by performing colorimetric measurements with a portable spectrophotometer CM-700d (Konica Minolta, Japan), with a white calibration standard Konica Minolta CM-A177. Measurements were taken in SCI mode (specular component included), using a measurement area of 8 mm diameter, a measurement range of 360–700 nm, under D65 illuminant and a 10° observer.

A total of 9 measurements were taken for each test Section (3 measurement points, 3 measurements per point). The mean values and standard deviations of the three color components (L, a*, and b*) and of the overall color change (ΔE) were calculated. The color differences of each component before and after laser treatment were then computed.

3.2.2. Roughness measurements

A SJ-210 portable profilometer (Mitutoyo, Japan) was used to perform surface roughness measurements. This instrument operates through a diamond-tipped stylus which moves along the surface and detects micro-irregularities. The stylus tip has a radius of 2 μm and the detector measuring force is 0.75 mN. In this study, data were collected according to ISO 4287: 1997, using a R-profile, a gaussian filter and a sampling length of 0.8 mm for 5 measurements, for a total of 4 mm. A short cut-off (λs) value of 2.5 μm was selected to eliminate high-frequency components such as noise.

Three replicates were performed for each measurement, and the mean surface roughness was evaluated before the application of the overlapping layer and after its removal, as well as the change in surface roughness.

3.2.3. Area extrapolation through photoshop software

An area extrapolation method was used to quantify the transformations induced on the surface by the laser beam. Each test section was photographed under consistent conditions, and the images were imported into Photoshop. With the software, it was possible to map the areas where the paint layer was exposed but altered, where residues of the overlapping layer remained, and where the paint layer appeared intact. The mapping was carried out by defining the RGB value of the non-altered pictorial layer through the *color range* tool. A tolerance value of 50 was applied in order to include the intrinsic chromatic heterogeneity of the pictorial layer while avoiding the selection of the clearly altered areas. The residual overlapping layer was mapped through a progressive selection using the *magic wand tool* with a tolerance value of 5. This methodology permitted the inclusion of the only visually detectable residues while minimizing the selection of the pictorial layer. The altered area was obtained as a subtraction between non-altered area and residual overlapping layer from the total surface. The three areas were transformed into different layers, allowing the number of pixels in each to be calculated and thus the total percentage of surface transformation to be quantified. This methodology was applied to all images to ensure consistency of the procedure.

3.3. Experimental plan and data treatment

3.3.1. The designed variables

In this study, two experimental investigations were carried out following the Design of Experiments (DoE) methodology, each aimed at removing a different overlapping layer, namely the *limewash* and the *strappo glue*.

The Design of Experiment adopted in this study is a four-factorial design, exploring the effects of the repetition rate (x_1), pulse duration (x_2), power (x_3), and scan speed (x_4). A specific range (minimum and maximum) was preliminarily selected for each parameter, and the defined ranges are reported in Table 2.

From a geometrical perspective, the four-factorial design explores the vertices of a geometric space called a hypercube. For 4 variables, the factorial design requires 2^4 experiments to be performed, corresponding to the corners of this figure. Additionally, a series of experiments are performed at the center of the hypercube to assess the reproducibility and the trend in the curves [32]. These experiments were performed in a randomized order to avoid cumulative error. For each study, a total of 19 cleaning tests were carried out at selected combination of parameters according to the DoE approach. Of these, 16 experiments correspond to the corner points of the hypercube and 3 to its center. Calculations were carried out using the CAT (Chemometric Agil Tool) software [51].

Table 2
Operation range of the parameters.

Overlapping layer	Studied parameters ranges				Fixed parameters	
	Repetition rate (kHz)	Pulse duration (ns)	Power (%)	Scan speed (m/s)	Scan shape	Dimension of scan shape (mm)
Limewash	350–700	2–6	50–100	1–5	Line	10
Strappo glue	40–90	30–80	50–100	6–13	Brush	20 fill: 0.95 mm, width: 100%

The model construction involves arranging the selected parameter values into a matrix, where each parameter is normalized to a range from −1 to +1. The experimental procedure ultimately provides a mathematical model describing the system behavior:

$$y = b_0 + b_1 x_1 + b_2 x_2 + b_3 x_3 + b_4 x_4 + b_5 x_1 x_2 + b_6 x_1 x_3 + b_7 x_1 x_4 + b_8 x_2 x_3 + b_9 x_2 x_4 + b_{10} x_3 x_4$$

where x_1, x_2, x_3 and x_4 represent the variables and each coefficient b_i carries a specific sign, a significance and an absolute value. The absolute value of the coefficient indicates the estimated effect of a variable on the response and so indicates which parameters are the most impactful, the sign expresses whether the variable has an increasing or decreasing effect on the response, according if its positive or negative. Furthermore, each coefficient has its own statistical significance expressed as a p-value.

3.3.2. The responses

A set of responses were selected to evaluate the outcome of each cleaning test.

The colorimetric analysis was employed to provide an analytical description of the color variation before and after cleaning. The variation of the three components L*, a*, and b* as well as the total perceptible difference ΔE were selected as responses for the Design of Experiment. The variation of the mean roughness, before and after the application of the overlapping layer and the laser treatment, was also selected as a response. Finally, the percentage of alteration of the paint layer, calculated using the area extrapolation method presented in paragraph 2.3.1, was also considered.

For the limewash samples, the measured values of ΔL, Δa, Δb, ΔE, and Δr showed no significant differences between the uncleaned test areas and those exhibiting alteration. Thus, to ensure a consistent interpretation within the Design of Experiment, the signs of the results corresponding to the uncleaned test sections were inverted, so that all responses followed the same directional logic (i.e., increasing values correspond to greater alteration).

3.3.3. Principal component analysis (PCA)

Principal Component Analysis (PCA) is a chemometric tool for transforming complex, multidimensional data into a more interpretable form by reducing its dimensionality [52].

In this study, Principal Component Analysis (PCA) was applied to the response variables obtained from the *limewash* and *strappo glue* removal tests.

To calculate the PCA models, the data must first be entered into a matrix, with each row representing a cleaning test and each column corresponding to the response values that reflect the outcome of the tests (see paragraph 2.3.2). The data were autoscaled and models were calculated using CAT (Chemometric Agil Tool) software [51]. The aim was to identify patterns, to group responses with similar characteristics, and to highlight the correlations between the responses. In the loading plots, responses with a strong correlation are positioned close together in the spatial domain, whereas responses inversely correlated have an opposite spatial orientation. In contrast, distant responses present different features and so different information.

For each resulting group, the response showing the highest significance, based on the percentage of explained variance provided through the DoE, was selected for further analysis.

4. Results and discussion

4.1. Experimental domain definition

For each of the two overlapping layers tested, a specific experimental domain was defined by selecting the ranges over which the four investigated parameters were explored (see Table 2). The two experimental domains selected differ because prior tests demonstrated that the two materials are removed at different and non–interchangeable parameter combinations. The two observed mechanisms also differ: the *limewash* removal is achieved by applying a point of water before the laser irradiation and through its instantaneous detachment from the surface. Instead, the removal of the *strappo glue* requires its gradual heating, swelling and consequent detachment from the surface. In both cleanings the removal was completed mechanically with the aid of a bamboo stick.

The prior experiments conducted demonstrated that the pulse duration range in which the *limewash* removal was achieved was between 2 and 6 ns, while for the *glue* removal the ideal range was defined at higher pulses duration, specifically from 30 to 80 ns. This result depends on the different ablation mechanisms involved according to the different pulse duration. [19,53] Furthermore, the tests conducted by varying the repetition rate revealed that different cleaning results could be achieved by modifying this parameter. Specifically, the removal of the *limewash* was accomplished at repetition rates in the hundreds, with the selected range being 350–700 kHz. The removal of the *glue,* instead, was favored at lower repetition rates, typically below 100 kHz, and the chosen range was 40–90 kHz. The variation in power percentage modulates the amount quantity of energy that is irradiated onto the material and, in the present study, a range of 50–100% was selected for both the *limewash* and the *strappo glue* removal. Finally, the scan speed is a key parameter in this laser application. Indeed, the *limewash* removal can only be achieved at low scan speeds. Thus, the range selected for the *limewash* removal is 1–5 m/s. For the *strappo glue* removal, a more gradual flow of energy was preferable so the range 6–13 m/s was selected. Indeed, a too short scan speed would result in the immediate burning of the glue, without allowing it to swell and detach.

Although the scan shape and dimensions were not included in the Design of Experiment and were instead preliminarily selected, they play a fundamental role in the cleaning process. For the *limewash* removal, a *line* scan shape with 10 mm size was preferred, while for the *strappo* glue the selected shape was the *brush*, with a width of 100%, a fill of 0.95 mm and a overall dimension of 20 mm. The choice of these two different combinations of shape and dimension is due to the fact that, for the same time, the *line* at 10 mm delivers more energy than the *brush* 20 mm, favoring the detachment of the *limewash.* Conversely, the *strappo glue* was removed though a more progressive and widespread delivery of energy. This preliminary selection helped to reduce the number of variants in the Design of Experiment, resulting in a more focused approach.

Once the experimental domain and the cleaning methodology were defined, the experiments were carried out in a randomized order, as described in Section 2.3.1, and all response variables were measured. A limitation of the methodology applied is that it does not account for the influence of local variations in the substrate, such as porosity, or any impurities present in the pigment composition, which could lead to variations in the cleaning results.

4.2. Screening of the responses through principal component analysis

As previously mentioned, a PCA model was built for each experiment to investigate the relationships among the response variables. The results obtained are presented below.

4.2.1. Strappo glue

The loading plot (Fig. 1a) highlights a clear grouping on PC1 and PC2, with an explained variance of 88.7% on PC1 and 6.7% on PC2. The spatial distribution of the responses on the loading plot reveals three distinct groups: (1) Δa and Δb, (2) ΔE and (3) the alteration

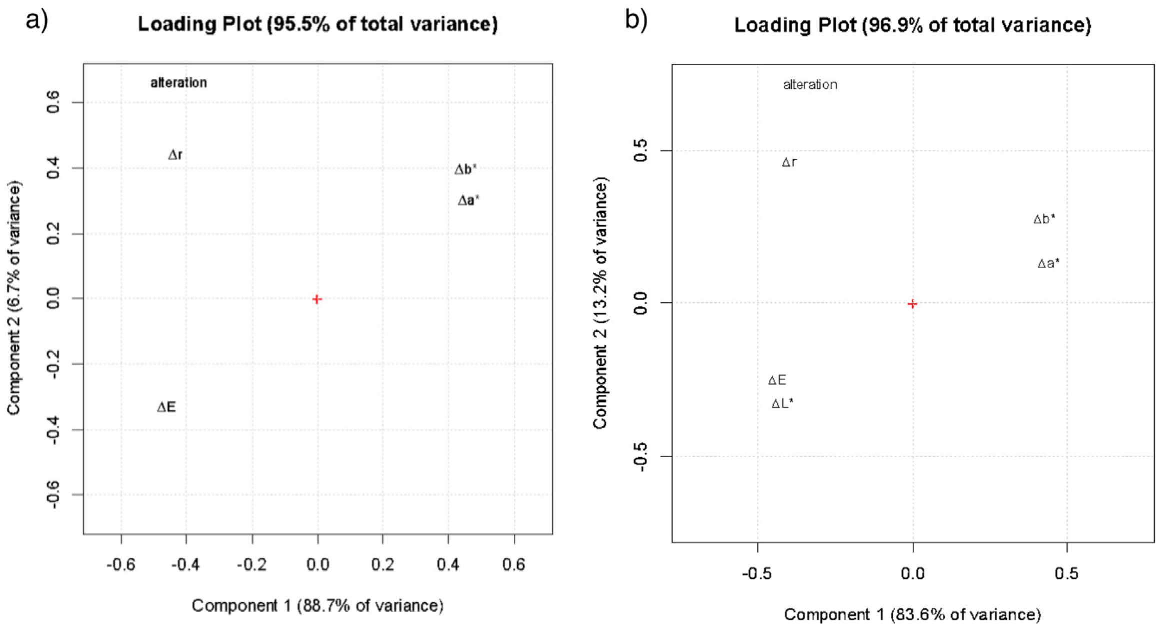

Fig. 1. Principal component analysis, loading plot: a) *strappo glue*, b) *limewash*.

and Δr. However, the Δa and Δb are inversely correlated with ΔE, indicating that they carry similar information.

Principal Component Analysis was used to assess the correlations among the selected response variables, revealing that analyzing all of them would result in redundant information. Based on the loadings plot, only a subset of variables was retained for experimental design modelling, specifically Δb and Δr.

4.2.2. Limewash

The loading plot (Fig. 1b) explains the 96.9% of the total variance, with 83.6% on PC1 and 13.2% on PC2. The analysis of the loading plot distribution clearly identifies the presence of four main groups: (1) Δa and Δb, (2) ΔE and ΔL, (3) Δr and (4) alteration.

Groups (1) and (2) appear to be inversely correlated and thus express similar information, while groups (3) and (4), while still retaining similar features, exhibit some differences that warrant further consideration.

In this case too, PCA assisted in selecting the variables to be studied within the DoE, choosing Δr and Δa, together with alteration.

4.3. The design of experiment responses

For each selected response, the values and statistical significance of the coefficients, together with the proportion of variance explained by the model (R^2), are reported in Table 3. The number of significant figures are reported according to the guidelines of Olivieri et al. [54].

4.3.1. Strappo glue

*4.3.1.1. Variation of the color component *b.* Through the study of the coefficients of the equation resulting from the Design of Experiment approach it was possible to define the parameters that influence the most the cleaning process, and those that increase and decrease the response effect. The most significant parameters affecting the b* component are the ones with a higher coefficient: pulse duration, power, and interaction between repetition rate and pulse duration, as well as the interactions of repetition rate-power, repetition rate-scan speed and pulse duration-power. Also the repetition rate and the interplay between pulse duration and power exhibit a notable role in the variation of b*.

It emerged that increasing repetition rate, pulse duration and power lead to more significant effects on the mock-up surface, whereas a faster scan speed results in a decrease in the cleaning efficiency.

The results demonstrate that by selecting the correct parameter combination is possible to achieve an ideal cleaning result, while an incorrect selection may lead to different forms of alterations (Fig. 2). Analysis of the response surfaces (Fig. 3) highlights that all the resulting surfaces exhibit a steep slope, indicating that an excessive increase in each parameter may lead to a compelling color variation. This is particularly significant for the variation of pulse duration and power, the two parameters that mostly affect this response variation, especially when the others are already at their maximum. The repetition rate, instead, does not have a compelling role in achieving the right conditions for the *glue* removal; however, it becomes significant in causing chromatic alteration at higher values, especially when the other parameters (such as power and pulse duration) are increased (Fig. 4). Indeed, the interaction between power and repetition rate (Fig. 3a) shows that the variation in the repetition rate is not significant at low power values, while it becomes significant at higher ranges by burning the *glue* and/or altering chromatically the paint layer. Overall, the variation of this parameter may be useful for modulating the cleaning once selected a suitable value of power and pulse duration. To remove the *glue,* a higher scan speed is preferable, because a slower scan speed may result in the immediate burning of the glue, without allowing it to swell and detach.

4.3.1.2. Roughness variation. As observed for the Δb variation, the analysis of the roughness variation response shows that pulse duration and power are the parameters with a highest coefficient, together with the interaction of repetition rate and scan pulse duration. Scan speed and the interaction between pulse duration and power also influence the outcome, although in a less meaningful way than the parameters previously mentioned.

As already said, pulse duration and power are the parameters that most influence *glue* removal and, when selected correctly, they

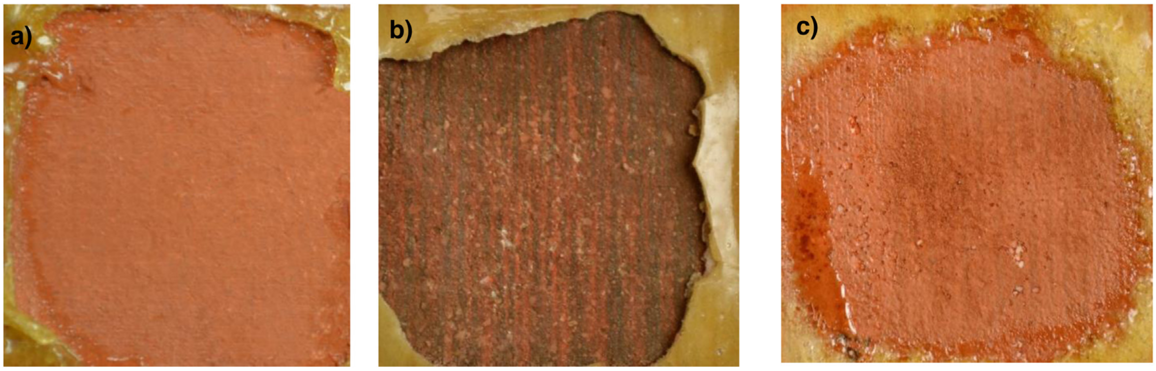

Fig. 2. Test sections of the *strappo glue* removal: a) pulse duration and power appropriately modulated, good result; b) high pulse duration and power, thinning of the paint layer; c) low scan speeds and high repetition rates, scan marks are visible on the surface.

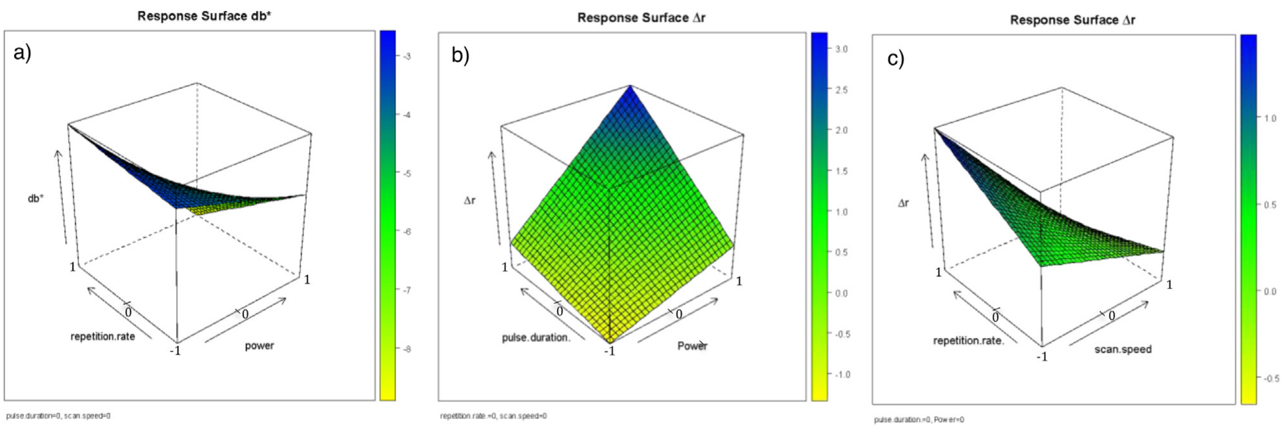

Fig. 3. *Strappo glue* removal. Response surfaces of: a) variation of color component *b, interaction between repetition rate and power; b) variation of the mean roughness, interaction between pulse duration and power; c) variation of the mean roughness, interaction between repetition rate and scan speed. Graph x and y axes are scaled within the range of −1 to +1 while the z-axis denotes the predicted response in its original units of measurement.

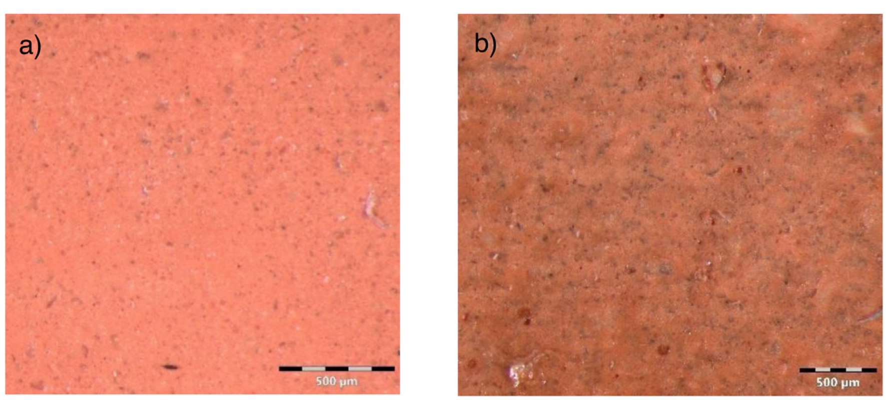

Fig. 4. Microscopic observation of the pictorial layer: a) before laser irradiation; b) after laser irradiation, with chromatic alteration of the surface due to high repetition rates.

enable effective cleaning without altering the surface morphology. Nevertheless, if selected at too high values, they can lead to the variation in the roughness of the paint layer, as confirmed by the steep slope of the response surface of the interaction of these two parameters (Fig. 3b). In comparison with the result obtained for Δb, the repetition rate appears here to be less significant. Indeed, in the *glue* removal, the repetition rate has a more relevant role in the eventual chromatic alteration rather than the actual variation of surface roughness. Conversely, the role of scan speed has a more dominant role on the variation of the roughness response than on the color variation, as a low scan speed can lead to visible scanning marks on the surface that correspond to the scan path selected. Indeed, the interaction between scan speed and repetition rate evidence that, at low scan speeds, the variation in the repetition rate notably affects the outcome, potentially leading to surface markings (Fig. 2c). In contrast, at high scan speeds, the influence of the variation in the repetition rate is negligible (Fig. 3c).

4.3.2. Limewash

4.3.2.1. Roughness variation. Among the investigated parameters, pulse duration emerges as the most impactful with a higher coefficient, with repetition rate and scan speed also playing substantial roles. In addition, the interaction between repetition rate and scan speed is particularly significant. Furthermore, power, together

Table 3
Value and statistical significance of the coefficients and R^2 of each model. The stars indicate the significance of the coefficients according to the convention * = $p < 0.05$, ** = $p < 0.01$, *** = $p < 0.001$.

	Response	b_0	Repetition rate (x_1)	Pulse duration (x_2)	Power (x_3)	Scan speed (x_4)	$x_1{\times}x_2$	$x_1{\times}x_3$	$x_1{\times}x_4$	$x_2{\times}x_3$	$x_2{\times}x_4$	$x_3{\times}x_4$	R^2 (%)
Strappo Glue	Δ*b	−4,99 (***)	−0,76 (**)	−1,56 (***)	−2,02 (***)	+0,45 (*)	+1,31 (***)	−1,14 (***)	+1,00 (***)	−0,72 (**)	−0,39 (/)	+0,08 (/)	95,67
	Δr	+0,3 (/)	+0,1 (/)	+1,1 (**)	+1,2 (**)	−0,7 (*)	−1,1 (**)	+0,0 (/)	−0,4 (/)	+0,6 (*)	−0,0 (/)	−0,1 (/)	78,88
Limewash	Δr	+0,33 (*)	+1,75 (***)	+2,64 (***)	+0,92 (***)	−1,44 (***)	+0,51 (**)	+0,63 (**)	−1,32 (***)	+0,62 (**)	−0,19 (/)	−0,37 (*)	97,54
	Alteration	+17 (***)	+16 (***)	+14 (***)	+7 (**)	−3 (/)	+11 (***)	+5 (*)	−4 (/)	+5 (/)	+1 (/)	−1 (/)	88,52
	Δ*a	+1 (/)	−8 (*)	−19 (***)	−5 (/)	+3 (/)	+2 (/)	+1 (/)	+4 (/)	−3 (/)	−8 (*)	+1 (/)	79,17

with other interactions such as repetition rate–pulse duration, repetition rate–power, and pulse duration–power exert a noticeable influence, although their individual effects are less dominant compared to the others.

Consistently with what previously demonstrated, a correct combination of parameters permits an adequate removal of the *limewash* without altering the underlying pictorial layer. Once again, it is important to emphasize the need to set the parameters correctly in order to avoid damaging the surface.

As previously demonstrated in the context of the *strappo glue* removal, the analysis of the coefficient signs revealed that higher repetition rates, pulse durations and power levels are associated to a major cleaning efficiency, whereas higher scan speeds decrease it.

An inversion in the roles of the repetition rate and the power is observed in the removal of *strappo glue* and *limewash.* For the *strappo glue*, power was a crucial parameter to achieve the desired cleaning outcome, while the repetition rate was mainly used for fine-tuning. Conversely, for *limewash*, repetition rate plays a key role and must be set above a certain threshold to enable an effective removal, as shown in Fig. 5a,b. In contrast, power has a limited impact, especially at low repetition rates or short pulse durations, but it may be effectively used to modulate the cleaning once the other parameters have been selected (Fig. 6a). The pulse duration significantly contributes to the overall effect, and so it is recommended to closely monitor its variation, especially when the repetition rate is already high, to avoid thinning of the paint layer (Fig. 5c). This finding is consistent with the results previously discussed on the role of the pulse duration in the removal of *strappo glue.* As highlighted by the response surfaces of the scan speed (Fig 6b), an effective removal of the *limewash* occurs at low scan speeds due to the major energy concentration, whereas at higher scan speeds this type of removal is more difficult to achieve. Therefore, it is advisable to operate at a low scan speed while modulating the other parameters. This result highlights how scan speed needs to be adjusted accordingly to the overlapping layer to be removed: while low scan speeds are required for the *limewash* removal, higher scan speed are preferable for the *strappo glue.*

4.3.2.2. Alteration of the surface. Within the examined variables, repetition rate and pulse duration are the parameters with highest coefficient, although the interaction between pulse duration and repetition rate with power is also noteworthy. Lastly, also the interaction between repetition rate and power must be taken into consideration, even if it appears to be less significant than the other interactions.

Analysis of the response surface demonstrates that it is possible to achieve the correct removal of the overlapping layer without inducing surface alterations when selecting an appropriate parameter combination. Nevertheless, the steep slope of the response surface of the interaction between repetition rate and pulse duration (Fig. 6c) highlights that, if increased excessively, alterations on the surface may be induced. Therefore, it may be useful to increase only one parameter at a time rather than immediately bringing them to their maximum. Although the scan speed has a high significance in the Δr response, as it plays a crucial role in the capability of achieving the right conditions for the removal of the *limewash,* its variation does not significantly affect the formation of alterations on the surface. Indeed, only when repetition rate and pulse duration are high and scan speed is low, it is possible to observe traces of the scan on the surface (Fig. 5d).

*4.3.2.3. Variation of the color component *a.* The developed model confirms the fundamental role of pulse duration in influencing the color variation in *limewash* removal, although also repetition rate and the interaction between pulse duration and scan speed emerge

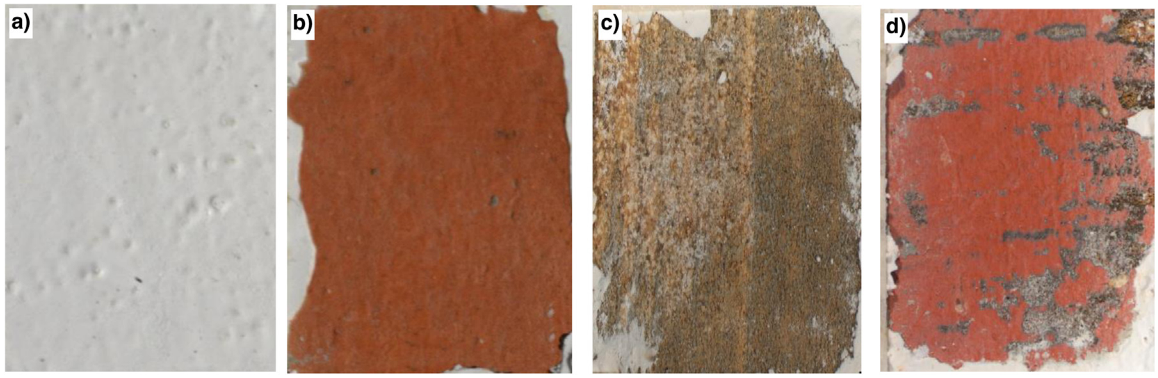

Fig. 5. Test sections of the *limewash* removal: a) test performed at low repetition rate, intact limewash layer; b) test performed above the repetition rate threshold, good result; c) thinning of the pictorial layer due to high pulse duration; d) the alteration follows the scan lines, that appear as horizontal parallel lines.

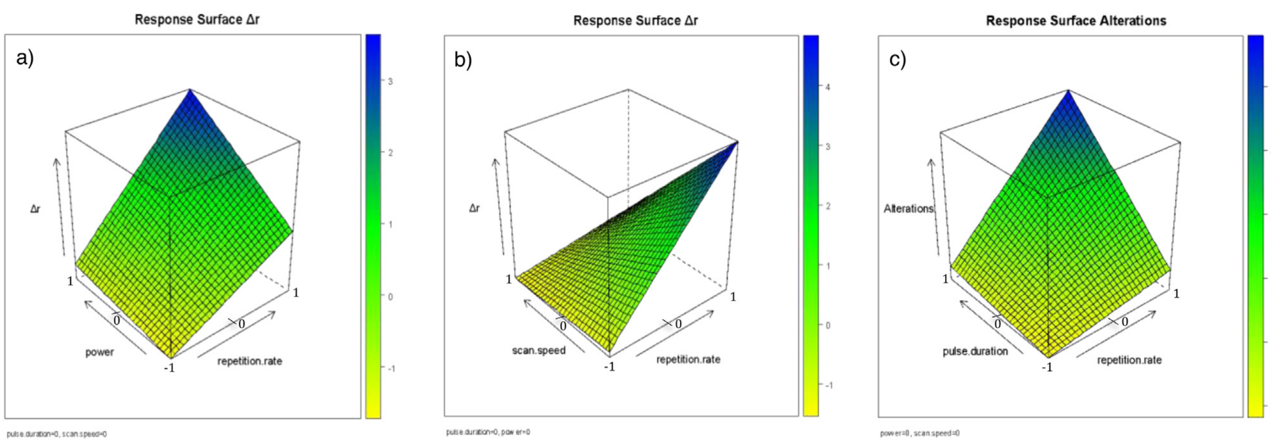

Fig. 6. *Limewash* removal. Response surfaces of: a) variation of the roughness, interaction between power and repetition rate; b) variation of the roughness, interaction between scan speed and repetition rate; c) formation of alterations, interaction between pulse duration and repetition rate. Graph x and y axes are scaled within the range of −1 to +1 while the z-axis denotes the predicted response in its original units of measurement.

as particularly meaningful. Instead, compared to the model obtained for the Δr and alteration responses, scan speed and power are less significant.

The evaluation of the interaction between pulse duration and repetition rate is essential to define a correct parameter selection that does not induce variation of the color component a*. At low repetition rates, power changes do not affect Δa variation; however, at high repetition rates and longer pulses the effect of power is significant.

5. Conclusions

This study proposes an innovative methodological approach that combines two chemometric tools, the Design of Experiments (DoE) and Principal Component Analysis (PCA) to investigate the influence of the adjustable parameters, namely repetition rate, pulse duration, power and scan speed, on the active fiber laser cleaning. The aim of this study was not to define a single optimal combination of laser parameters for the removal of the *strappo glue* and the *limewash,* as each artwork presents unique materials and conservation conditions, but rather to achieve an in-depth understanding of the underlying experimental dynamics. Indeed, the integrated PCA-DoE approach allowed a systematic evaluation of parameter effects and interactions, clarified which variables govern the desired cleaning mechanisms, which may be used for fine-tuning, and which combinations may induce unwanted surface modifications when improperly selected. Differences in the removal behavior of inorganic and organic materials were also highlighted.

The good cleaning results demonstrate the effectiveness of this laser technology in removing two different overlapping layers and its capability to preserve a sensitive and delicate substrate, recommending further development of this technology in the conservation field. Furthermore, the results highlight the great effectiveness of this laser system, that requires a careful parameter modulation to obtain the desired cleaning effect.

A key advantage of the DoE methodology is that it enables the experimental domain and the total number of tests to be defined a priori, before performing the actual cleaning experiments. This aspect is particularly valuable in any experimental context, as it allows the required time, resources, and effort to be estimated in advance, while ensuring that the minimum number of experiments necessary to extract statistically meaningful information is performed. Moreover, DoE makes it possible to investigate the influence of the selected parameters over the entire experimental domain, rather than being limited to discrete tested conditions. PCA was subsequently applied to analyze the experimental responses, identify correlations among them, and rationalize the dataset by selecting a representative subset of response variables. This step significantly simplified data interpretation and enabled a clearer understanding of the relationships between process parameters, cleaning efficiency, and potential surface alterations.

The proposed approach is inherently suitable for optimization tasks, thus fulfilling a dual purpose: enabling comprehensive investigation of complex laser-cleaning processes while also providing a robust framework for identifying optimal parameter combinations tailored to specific case studies in cultural heritage conservation.

Funding

This research was funded by the European Union–NextGenerationEU (PhD in cooperation with industrial partners—M4C2 I. 3.3) and El.En. Group.

Acknowledgments

M.P and D.S. acknowledge support from the Project CH4.0 under the MUR program “Dipartimenti di Eccellenza 2023–2027” (CUP: D13C22003520001).

References

[1] J.F. Asmus, C.G. Murphy, W.H. Munk, Studies on the interaction of laser radiation with art artifacts, in: R.F. Wuerker (Ed.), Developments in Laser Technology II, SPIE, 1974, pp. 19–30, doi:10.1117/12.953831.
[2] M. Cooper, Laser Cleaning in Conservation: An Introduction, Butterworth-Heinemann, Woburn, MA, 1998.
[3] S.D. Dondieu, K.L. Wlodarczyk, P. Harrison, A. Rosowski, J. Gabzdyl, R.L. Reuben, D.P. Hand, Process optimization for 100 w nanosecond pulsed fiber laser engraving of 316l grade stainless steel, J. Manuf. Mater. Process. 4 (2020) 110, doi:10.3390/jmmp4040110.
[4] T.T. Vu, H.H. Hoang, Investigating the effect of pulsed Fiber laser parameters on the roughness of aluminium alloy and steel surfaces in cleaning processes, Lasers Manuf. Mater. Process. 8 (2021) 113–124, doi:10.1007/s40516-021-00139-1.
[5] J. Hildenhagen, K. Dickmann, Innovative approaches in laser cleaning researches and instrumentation development the effect of ultrafast lasers on laser cleaning: mechanism and practice, in: R. Radvan, J.F. Asmus, M. Castillejo, P. Pouli, A. Nevin (Eds.), Lasers in the Conservation of Artworks VIII, CRC Press, London, 2010, pp. 21–26, doi:10.1201/b10567-6.
[6] B. Graue, S. Brinkmann, C. Verbeek, PROCON TT 49: laser cleaning of ancient Egyptian wall paintings and painted stone surfaces, in: J.F. Asmus, M. Castillejo, P. Pouli, A. Nevin (Eds.), Lasers in the Conservation of Artworks VIII, CRC Press, London, 2010, pp. 65–70, doi:10.1201/b10567-12.
[7] A. Suzuki, C. Riminesi, M. Ricci, S. Vettori, B. Salvadori, Testing of a new Yb:YAG fiber laser system for the removal of graphic vandalism from marble, Herit. Sci. 11 (2023), doi:10.1186/s40494-023-00966-9.
[8] A. Faron, M. Iwanicka, Preliminary study and implementation of nanosecond NIR fibre laser in conservation of polychrome heritage objects, in: S. Siano, D. Ciofini (Eds.), Lasers in the Conservation of Artworks XIII, CRC Press, London, 2024, pp. 104–112, doi:10.1201/9781003386872-11.
[9] A. Dajnowski, T.J. Tague Jr., T. Roberts, M. Strutt, B.A. Price, N.M. Kelly, D.W. Tague, K.R. Sutherland, B.A. Dajnowski, You can clean but cannot touch. Graffiti removal from prehistoric pictographs at Hueco Tanks State Park & Historic Site using laser ablation process, in: S. Siano, D. Ciofini (Eds.), Lasers in the Conservation of Artworks XIII, CRC Press, London, 2024, pp. 96–103, doi:10.1201/9781003386872-10.
[10] F. Surma, P. Schloegel, V. Aguilar, L. Rosenbaum, M. Labouré, Laser cleaning of graffiti and cleaning evaluation, in: Lasers in the Conservation of Artworks XIII, CRC Press, London, 2024, pp. 219–228, doi:10.1201/9781003386872-23.
[11] M. Polizzi, F. Zenucchini, C. Ricci, A. Segimiro, Rimozione di ridinture non originali da una statua in gesso con un laser in fibra attiva 300W, in: Applicazioni Laser Nel Restauro APLAR 8, Nardini Editore, Florence, 2025, pp. 245–255.
[12] F. Zenucchini, C. Ricci, A. Piccirillo, P. Luciani, Confronto tra sistemi laser a fibra attiva per la pulitura di superfici dei beni culturali in legno non policromo, in: Applicazioni Laser Nel Restauro APLAR 8, Nardini Editore, Florence, Italy, 2025, pp. 97–108.
[13] A. Kerr, B. Dajnowski, Development and application of a custom green laser system to remove decades old penciled graffiti on raw canvas from Morris Louis' masterwork, Beta Upsilon, in: S. Siano, D. Ciofini (Eds.), Lasers in the Conservation of Artworks XIII, CRC Press, London, 2024, pp. 163–172, doi:10.1201/9781003386872-17.
[14] E. Di Francia, R. Lahoz, D. Neff, E. Angelini, S. Grassini, Laser cleaning of Cu-based artefacts: laser/corrosion products interaction, Acta IMEKO 7 (2018) 104, doi:10.21014/acta_imeko.v7i3.610.
[15] A. Dajnowski, B.A. Dajnowski, Using the new G.C. laser cleaning system for cleaning and surface preparation for re-gilding of a large outdoor bronze monument of Alexander Hamilton, in: P. Targowski, M. Walczak, P. Pouli (Eds.), Proceedings of the International Conference LACONA XI, Nicolaus Copernicus University Press, Toruń, 2017, pp. 217–228, doi:10.12775/3875-4.15.
[16] M.-C. Canepa, F. Zenucchini, R.M.A. Coco, A. Piccirillo, P. Manchinu, L. Apollonia, M. Cardinali, Applicazioni laser su superfici lapidee di grandi dimensioni: tempi di applicazione e risultati a confronto, in: Applicazioni Laser Nel Restauro APLAR 7, Nardini Editore, Florence, 2022, pp. 203–219.
[17] M.P. Fiorucci, A.J. López, A. Ramil, S. Pozo, T. Rivas, Optimization of graffiti removal on natural stone by means of high repetition rate UV laser, Appl. Surf. Sci. 278 (2013) 268–272, doi:10.1016/j.apsusc.2012.10.092.
[18] S. Siano, R. Salimbeni, The gate of paradise: physical optimization of the laser cleaning approach, Stud. Conserv. 46 (2001) 269–281, doi:10.1179/sic.2001.46.4.269.
[19] S. Siano, Principles of laser cleaning in conservation, in: M. Schreiner, M. Strlič, R. Salimbeni (Eds.), Handbook on the Use of Lasers in Conservation and Conservation Science, COST Office, Brussels, 2008.
[20] L. Bartoli, P. Pouli, C. Fotakis, S. Siano, R. Salimbeni, Characterization of stone cleaning by Nd:YAG lasers with different pulse duration, Laser Chem. 2006 (2006) 1–6, doi:10.1155/2006/81750.
[21] R. Salimbeni, R. Pini, S. Siano, A variable pulse width Nd:YAG laser for conservation, J. Cult. Herit. 4 (2003) 72–76, doi:10.1016/S1296-2074(02)01149-4.
[22] G. Zhu, Z. Xu, Y. Jin, X. Chen, L. Yang, J. Xu, D. Shan, Y. Chen, B. Guo, Mechanism and application of laser cleaning: a review, Opt. Lasers Eng. 157 (2022) 107130, doi:10.1016/j.optlaseng.2022.107130.
[23] I. Bozsóki, B. Balogh, P. Gordon, 355 nm nanosecond pulsed Nd:YAG laser profile measurement, metal thin film ablation and thermal simulation, Opt. Laser Technol. 43 (2011) 1212–1218, doi:10.1016/j.optlastec.2011.03.011.
[24] R. Pini, S. Siano, Optical diagnostic systems and sensors to control laser cleaning of artworks, Opt. Sens. Microsyst. (2002) 267–274, doi:10.1007/0-306-47099-3_24.
[25] T. Bian, Y. Bai, L. Yu, Z. Xu, Laser cleaning of paint layers on white marble surface based on cooperative use of laser-induced breakdown spectroscopy and image binarization, J. Cult. Herit. 62 (2023) 124–133, doi:10.1016/j.culher.2023.05.018.
[26] L. Hou, F. Yin, S. Wang, J. Sun, H. Yin, A review of thermal effects and substrate damage control in laser cleaning, Opt. Laser Technol. 174 (2024) 110613, doi:10.1016/j.optlastec.2024.110613.
[27] J. Liu, P. Lü, Y. Sun, Y. Wang, Surface roughness and wettability of dentin ablated with ultrashort pulsed laser, J. Biomed. Opt. 20 (2015) 055006, doi:10.1117/1.jbo.20.5.055006.
[28] F. Brygo, C. Dutouquet, F. Le Guern, R. Oltra, A. Semerok, J.M. Weulersse, Laser fluence, repetition rate and pulse duration effects on paint ablation, Appl. Surf. Sci. 252 (2006) 2131–2138, doi:10.1016/j.apsusc.2005.02.143.
[29] G. Raciukaitis, M. Brikas, P. Gecys, M. Gedvilas, Accumulation effects in laser ablation of metals with high-repetition-rate lasers, High-Power Laser Ablation VII, SPIE, 2008, 70052L, doi:10.1117/12.782937.
[30] M.K.A.A Razab, M.S. Jaafar, A.A. Rahman, S. Mamat, M.I. Ahmad, F.M. Suhaimi, Influenced of threshold fluence, absorption coefficient and thermal loading in laser paint removal mechanisms, in: Environment, Energy and Applied Technology: Proceedings of the 2014 International Conference on Frontier of Energy and Environment Engineering (ICFEEE 2014), CRC Press, London, 2015.
[31] G. Zhang, X. Hua, F. Li, Y. Zhang, C. Shen, J. Cheng, Effect of laser cleaning process parameters on the surface roughness of 5754-grade aluminum alloy, Int. J. Adv. Manuf. Technol. 105 (2019) 2481–2490, doi:10.1007/s00170-019-04395-6.
[32] W. Zhuang, X. Yang, G. Xia, D. Li, W. Liu, J. Cheng, S. Wan, Effect of laser power on cleaning mechanism and surface properties, Appl. Opt. 59 (2020) 9482, doi:10.1364/AO.399691.
[33] J. Riu, B. Giussani, Analytical chemistry meets art: the transformative role of chemometrics in cultural heritage preservation, Chemom. Intell. Lab. Syst. 247 (2024) 105095, doi:10.1016/j.chemolab.2024.105095.
[34] A. Sarmiento, M. Pérez-Alonso, M. Olivares, K. Castro, I. Martínez-Arkarazo, L.A. Fernández, J.M. Madariaga, Classification and identification of organic binding media in artworks by means of Fourier transform infrared spectroscopy and principal component analysis, Anal. Bioanal. Chem. 399 (2011) 3601–3611, doi:10.1007/s00216-011-4677-0.
[35] G. Visco, E. Gregori, M. Tomassetti, L. Campanella, Probably counterfeit in roman imperial age: pattern recognition helps diagnostic performed with inductive coupled plasma spectrometry and thermogravimetry analysis of a torso and a head of roman age marble statue, Microchem. J. 88 (2008) 210–217, doi:10.1016/j.microc.2007.11.013.
[36] G. Sciutto, S. Prati, I. Bonacini, P. Oliveri, R. Mazzeo, FT-NIR microscopy: an advanced spectroscopic approach for the characterisation of paint cross-sections, Microchem. J. 112 (2014) 87–96, doi:10.1016/j.microc.2013.09.021.
[37] E. Marengo, M.C. Liparota, E. Robotti, M. Bobba, Monitoring of paintings under exposure to UV light by ATR-FT-IR spectroscopy and multivariate control charts, Vib. Spectrosc. 40 (2006) 225–234, doi:10.1016/j.vibspec.2005.09.005.
[38] E. Catelli, G. Sciutto, S. Prati, M.V. Chavez Lozano, L. Gatti, F. Lugli, S. Silvestrini, S. Benazzi, E. Genorini, R. Mazzeo, A new miniaturised short-wave infrared (SWIR) spectrometer for on-site cultural heritage investigations, Talanta 218 (2020) 121112, doi:10.1016/j.talanta.2020.121112.
[39] L. Geminiani, F.P. Campione, C. Canevali, C. Corti, B. Giussani, G. Gorla, M. Luraschi, S. Recchia, L. Rampazzi, Historical silk: a novel method to evaluate degumming with non-invasive infrared spectroscopy and spectral deconvolution, Mater. (Basel) 16 (2023) 1819, doi:10.3390/ma16051819.
[40] G. Pellis, M. Tiburziano, B. Giussani, P. Letardi, B. Salvadori, A. Sansonetti, D. Scalarone, Advancing preservation: a chemometric approach for monitoring the degradation of protective coatings for bronze statues, Microchem. J. 210 (2025) 112971, doi:10.1016/j.microc.2025.112971.
[41] C. Mazzuca, L. Micheli, F. Marini, M. Bevilacqua, G. Bocchinfuso, G. Palleschi, A. Palleschi, Rheoreversible hydrogels in paper restoration processes: a versatile tool, Chem. Cent. J. 8 (2014) 10, doi:10.1186/1752-153X-8-10.
[42] G. Sciutto, P. Oliveri, S. Prati, M. Quaranta, S. Bersani, R. Mazzeo, An advanced multivariate approach for processing X-ray fluorescence spectral and hyper-

spectral data from non-invasive in situ analyses on painted surfaces, Anal. Chim. Acta 752 (2012) 30–38, doi:10.1016/j.aca.2012.09.035.
[43] M. Dan, Using design of experiments for creating a conservation treatment for cultural heritage, within a university—industry collaboration project, in: Managerial Challenges of the Contemporary Society, Babes-Bolyai University, Cluj Napioca, 2021, pp. 117–122.
[44] J. Ouyang, P. Mativenga, N. Goffin, W. Liu, Z. Liu, N. Mirhosseini, L. Jones, E. Woolley, L. Li, Energy consumption and performance optimisation of laser cleaning for coating removal, CIRP J. Manuf. Sci. Technol. 37 (2022) 245–257, doi:10.1016/j.cirpj.2022.02.001.
[45] R. Leardi, Experimental design in chemistry: a tutorial, Anal. Chim. Acta 652 (2009) 161–172, doi:10.1016/j.aca.2009.06.015.
[46] M. Salvadori, C. Sbrolli, Wall paintings through the ages: the roman period—republic and early empire, Archaeol. Anthr. Sci. 13 (2021), doi:10.1007/s12520-021-01411-3.
[47] D. Jiménez-Desmond, J.S. Pozo-Antonio, A. Arizzi, The fresco wall painting techniques in the Mediterranean area from antiquity to the present: a review, J. Cult. Herit. 66 (2024) 166–186, doi:10.1016/j.culher.2023.11.018.
[48] L.C. Lancaster, Mortars and plasters—how mortars were made. The literary sources, Archaeol. Anthr. Sci. 13 (2021), doi:10.1007/s12520-021-01395-0.
[49] P. Mora, L. Mora, P. Philippot, La Conservazione delle Pitture Murali, Editrice Compositori, Bologna, 1999.
[50] Smart laser, light for art, (n.d.). https://www.lightforart.com/en/smart-laser-2/ (Accessed 13 December 2025).
[51] R. Leandri, C. Melzi, G. Polotti, CAT (Chemometric Agile Tool), freely downloadable, (n.d.). http://gruppochemiometria.it/index.php/software (Accessed 17 December 2025).
[52] S. Wold, K. Esbensen, P. Geladi, Principal component analysis, Chemom. Intell. Lab. Syst. 2 (1987) 37–52, doi:10.1016/0169-7439(87)80084-9.
[53] S. Siano, R. Salimbeni, Advances in laser cleaning of artwork and objects of historical interest: the optimized pulse duration approach, Acc. Chem. Res. 43 (2010) 739–750, doi:10.1021/ar900190f.
[54] A.C. Olivieri, Practical guidelines for reporting results in single- and multicomponent analytical calibration: a tutorial, Anal. Chim. Acta 868 (2015) 10–22, doi:10.1016/j.aca.2015.01.017.